

WINGLETS – MULTIOBJECTIVE OPTIMIZATION OF AERODYNAMIC SHAPES

SOHAIL R. REDDY¹, HELMUT SOBIECZKY², ABAS ABDOLI¹ AND
GEORGE S. DULIKRAVICH^{1*}

¹ Department of Mechanical and Materials Engineering, MAIDROC Laboratory, Florida International University, Miami, FL 33174, USA
{sredd001@fiu.edu, aabdo004@fiu.edu, dulikrav@fiu.edu} <http://MAIDROC.fiu.edu>

² University of Technology, Institute of Fluid Mechanics and Heat Transfer, Vienna, Austria
E-mail: helmut@sobieczky.at [Http://www.sobieczky.at/aero/](http://www.sobieczky.at/aero/)

Key Words: *Winglets, Aerodynamic Shape Design, Multi-Objective Optimization*

Abstract. Various configurations for airplane wing tip winglets have been investigated by performing 3D aerodynamic analysis. An existing blended winglet has been equipped with a secondary lower element to create a split winglet configuration. At winglet tips, a trailing edge extension was added to create scimitar streamwise spikes. A total of eight variables were used to define the winglet geometry. The presented design methodology utilizes a second order continuous, 3D geometry generation algorithm based on locally analytical surface patches. This algorithm requires a minimal number of design parameters to be varied in order to create vastly different 3D geometries of the winglets attached to a clean wing which is blended with the fuselage. A 3D, compressible, turbulent flow analysis was performed using a Navier-Stokes solver on each configuration to obtain objective function values. Each configuration was analyzed at free stream Mach number of 0.25 and an angle of attack of 11 degrees to mimic takeoff conditions of a passenger aircraft. Multi-objective optimization was carried out using modeFRONTIER utilizing a radial basis function response surface approximation coupled with a genetic algorithm. Maximizing coefficient of lift and lift-to-drag ratio, while minimizing coefficients of drag and magnitude of coefficient of moment, were the four simultaneous objectives. Performance benefits of individual components of the optimized geometry were also investigated.

1 INTRODUCTION

The constant need to improve aerodynamic efficiency of an aircraft is one of the challenges in the aerospace field. This led to the invention of wingtip devices called winglets in order to reduce aerodynamic drag. The pressure difference between the upper and lower wing surface tries to equalize itself by flowing around the wingtips causing vortices. These wingtip devices help break these wingtip vortices thereby reducing induced drag. Induced

drag is greatest in high lift scenarios such as takeoff and landings of aircraft, but is also significant at cruise conditions. This reduction in drag results in better fuel efficiency, lower emissions and greater range.

The aerodynamic induced drag is proportional to the radii of the wingtip vortices and the spacing between them [1]. The amount of drag induced by the aircraft can be significantly reduced by implementing a wingtip design that increases the radii of the vortices and distance between the vortices [2]. Over the years, various types of winglet designs have been explored including spiroid winglets [3], multi-winglets [4,5] and blended winglets [6]. However, there is very little known about split-scimitar winglets introduced by Aviation Partners in 2013.

The split-scimitar winglets feature a traditional blended winglet design retrofitted with a secondary lower ventral strake (Figure 1). Both the blended winglet and the ventral strake are capped with a blended-sweptback tip spike. The effects of each of these individual components were investigated in this work. A multi-objective optimization was carried out to find a design satisfying the four simultaneous objectives: minimize coefficient of drag and the magnitude of the coefficient of moment, and maximizing the coefficient of lift and lift-to-drag ratio.

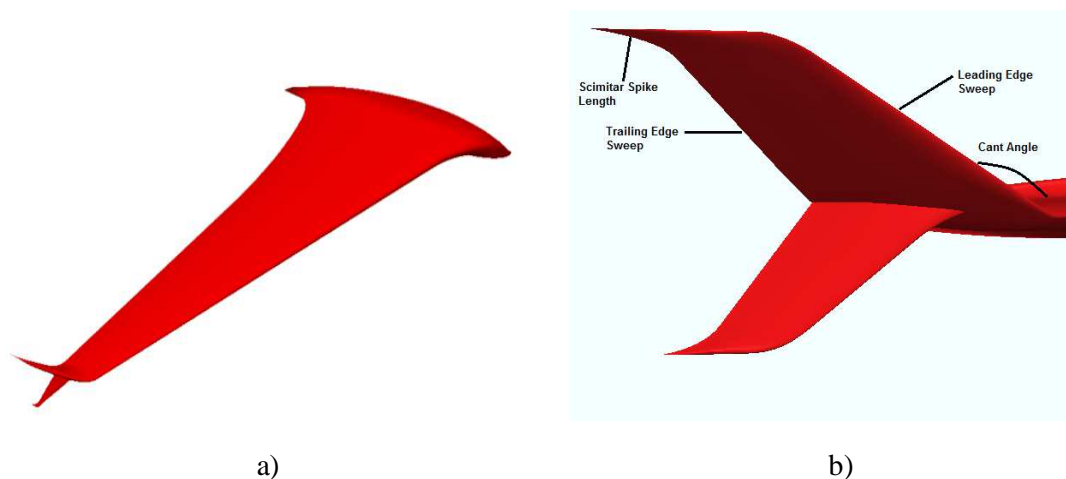


Figure 1: A Boeing 7E7 wing with a scimitar winglet (a) and some of the geometric design parameters for scimitar winglet (b).

Single winglets have previously been a topic of design optimization for various applications. Kubrynski presented a combined inverse shape design and optimization approach [7] which resulted in actual high performance awards winning sailplanes that used such horns-up blended winglets. This approach requires the user to be an experienced aerodynamicist especially because of the requirement to prescribe good pressure distribution on such winglets when performing an inverse shape design.

Bourdin *et al.* [8] performed experimental work on the effects of cant angle on winglet performance. Multi-disciplinary, multi-objective optimization has been carried out on single winglets by Takenaka *et al.* [9], Ursache *et al.* [10]. Weierman and Jacob [11] optimized blended winglets for UAV, while EnginSoft optimized winglets for the Piaggio Aero business jet [12]. A team of undergraduate mechanical engineering students at Florida International University [13] also performed multi-objective design optimization of a naked Boeing 757

wing with horns-up and horns-down winglets. Their work used Euler equations of 3D inviscid gasdynamics at free stream Mach number 0.3 and wing angle of attack of 8 degrees. Results of their work are summarized in Figure 2.

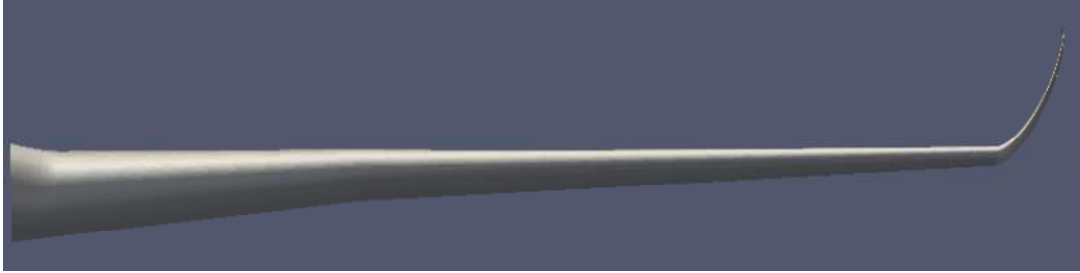


Figure 2: A Boeing 757 wing with the Pareto optimized horns-up winglet [13].

On the other hand, there is very little published on aerodynamic shape optimization of multi-winglets such as in Figure 1. Each winglet configuration in this study was analyzed using OpenFOAM [14] computational fluid dynamics software, while the optimization was performed using modeFRONTIER [15] with radial basis function based response surface approximation coupled with a genetic algorithm.

2 GEOMETRY DEFINITION

When performing aerodynamic shape design optimization, it is necessary to use an efficient method to define the geometry with a minimum number of parameters (design variables) to reduce computational cost. A flexible geometry generator with minimal number of parameters input drastically reduces the number of design variable, thus requiring a smaller initial population needed to create a response surface [16] for each of the for aerodynamic objectives. This study utilizes a FORTRAN code “E300” developed by Sobieczky [17,18].

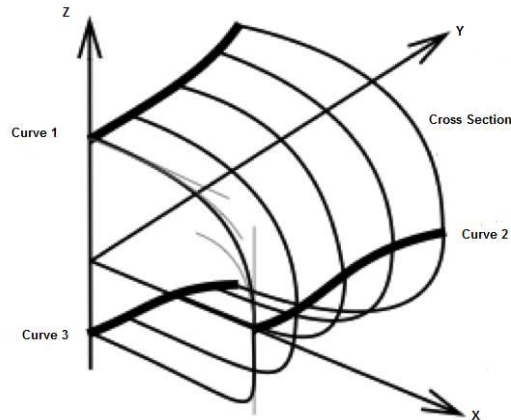


Figure 3: Surface definition using multiple guide curves

It utilizes analytical functions over an interval to define the surface. A piecewise composition of these functions yields a continuous curve with the user maintaining control over each segment. The curves can also be defined in three-dimensional space to control the extrusion of a cross section as shown in Figure 3.

We used this approach to control the eight parameters that defined the complete split (scimitar) winglet. Figure 1b shows these parameters applied to the upper element, but the study applies them to both the upper and lower element. The parameters used to define the complete split winglet geometry include the leading and trailing edge sweeps of both the upper and lower elements, tip spike lengths of both elements and the cant angle of both elements. Controlling the leading edge and trailing edge sweep independently allows for control over a third parameter, the taper ratio. Figure 1a shows the wing that was used for analysis of all of the winglet configurations. The wing was modeled after a Boeing 7E7 prototype. A symmetric PARSEC11 airfoil was used to define both the upper and lower elements of the split winglet.

Table 1 shows the allowable range for each of the eight design variables; four for the upper winglet and four for the lower winglet. The lengths of scimitar streamwise spikes were allowed to vary between 0, indicating no spike, and the length of the tip chord, where λ is some random number between zero and one. The tip chord is related to the taper ratio and therefore the leading edge and trailing edge sweeps.

Table 1: Design variables and their user-specified allowable ranges

Design Variable	Minimum Value	Maximum Value
Upper Leading Edge Sweep	35°	70°
Upper Trailing Edge Sweep	45°	85°
Upper Cant Angle	30°	85°
Upper Scimitar Spike Length	0	λ *Upper Tip Chord Length
Lower Leading Edge Sweep	35°	70°
Lower Trailing Edge Sweep	45°	85°
Lower Cant Angle	25°	85°
Lower Scimitar Spike Length	0	λ *Lower Tip Chord Length

3 AERODYNAMIC ANALYSIS

The objective functions (coefficients of lift, drag, moment and lift/drag) for each design were obtained by carrying out 3D fluid flow analysis in OpenFOAM [14]. OpenFOAM uses a Gaussian finite volume with hexahedral cells integration method for computation of derivatives. It makes use of a linear interpolation scheme. The SIMPLE (Semi-Implicit Method for Pressure-Linked Equations) algorithm was used to solve the Navier-Stokes equations. The standard $k-\epsilon$ turbulence model was used to capture flow separation, with standard no-slip and no penetration boundary conditions at the geometry.

Each 3D aerodynamic analysis run took approximately 9 hours if starting with a uniform flow as an initial guess, or 3 hours if the converged solutions from other wing+winglet configuration fields were used as initial guesses. A boundary-conforming hybrid computational grid of approximately 7 million grid cells was used for each of the randomly

generated wing+winglet configurations. Computation grid generation for each case took approximately one hour. A single processor was used for each case, with 16GB ram allocated per case. Currently, the computing cluster features 912 Intel based cores and a total memory of 2.8TB.

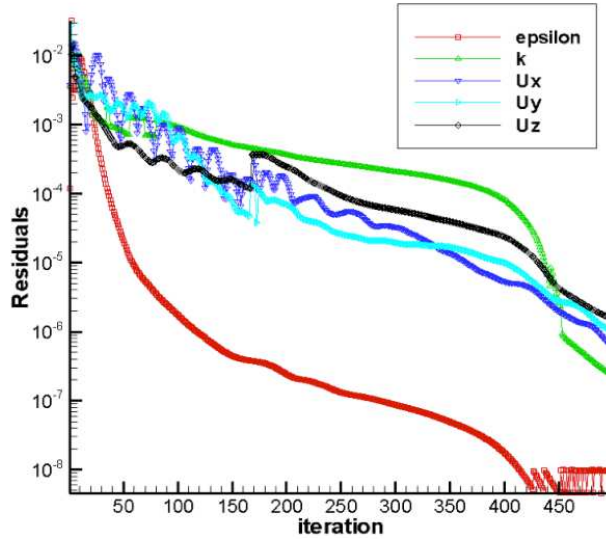


Figure 4. A typical convergence history of OpenFOAM aerodynamic analysis software.

As performance benefits of different configuration of winglets are being analyzed, a benchmark value is needed for comparison. The barren (naked) Boeing 7E7 wing without winglets was aerodynamically analyzed under these conditions: free stream Mach number of 0.25 and wing angle of attack of 11 degrees. Figure 4 represents a typical convergence history for 3D analysis runs in this study. It can be concluded that OpenFOAM aerodynamic analysis software converged fully, thus creating high fidelity values of the four aerodynamic coefficients to be optimized.

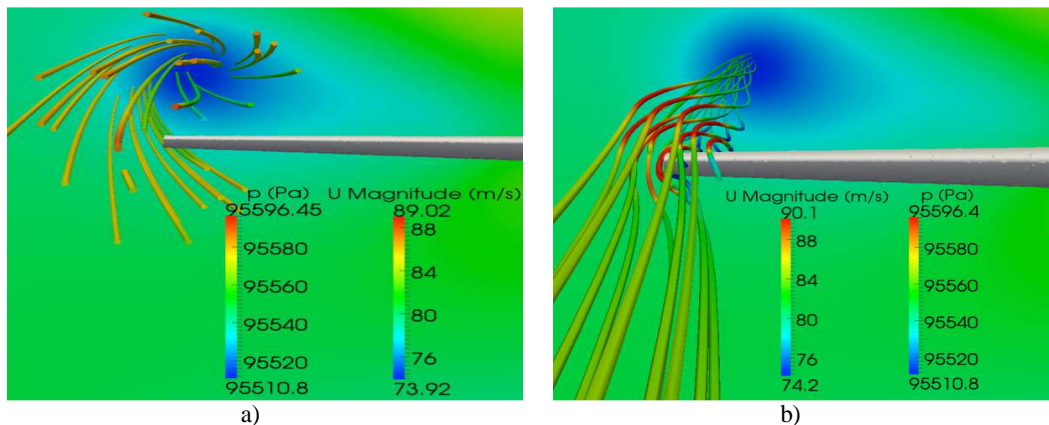


Figure 5: Streamlines moving inbound around a naked 7E7 wing depicted at: a) four chord lengths downstream of trailing edge, and b) 20 degree yaw angle.

A Trefftz plane perpendicular to the axis of the free stream was placed four chord lengths downstream of the wing's trailing edge, to visualize the low-pressure region created by the wing tip vortex (Figure 5a) in the case of a naked wing. Figure 5b shows an enlarged view of the streamlines around the wing tip of this naked wing. Color variation of the streamlines indicates the velocity magnitude along those streamlines. The radius of the vortex core is quite small as compared to designs incorporating winglets, as will be seen in the following figures.

4 OPTIMIZATION

The multi-objective optimization in this study was carried out with the commercial software modeFRONTIER [15]. Since each 3D aerodynamic analysis is computationally time consuming, an eight-dimensional (since there are eight geometric design variables in this study) response surface approximation based on Gaussian Radial Basis Functions (GRBF) was created for each of the four objectives that need to be extremized simultaneously: C_L , C_D , C_m and C_L/C_D . Colaco and Dulikravich [21] demonstrated that the GRBF method gives more accurate results as compared to other response surface methods. In the present study, the response surfaces were created by high fidelity results for the aerodynamic coefficients from only 40 different wing+scimitar winglet configuration analyses. Accuracy of the generated response surfaces was verified by comparing the aerodynamic coefficients' values obtained from interpolation on the response surface versus the results obtained with OpenFOAM code. The objective function values obtained from GRBF deviated by 2% from those obtained from OpenFOAM. Other response surface generation methods deviated by as much as 30%.

The response surfaces were then coupled with the genetic algorithm NSGA II (Non-Dominated Sorting Genetic Algorithm-II) optimizer developed by Deb *et al.* [22,23] that searched them to arrive at a Pareto frontier which represents a set of the best trade-off solutions since there is no unique optimum in case of multi-objective optimization. Optimization took only 30 minutes on a laptop computer and did not involve optimizing the 7E7 wing. That is, the 7E7 basic wing was unchanged during the entire optimization.

5 GENERAL WORKFLOW

The workflow used in this study is depicted in Fig. 6. The geometry is modeled using a set of analytical functions with parameterized input. This allows for precise control over the geometry while keeping the number of parameters needed to define the geometry at the minimum. A quasi-random number generator [19] was used to create an initial population of 40 candidate scimitar winglet configurations by randomly determining each of the eight design variables within their specified allowable ranges. Compressible, 3D turbulent flow analysis was then carried out with a free software OpenFOAM [14,20].

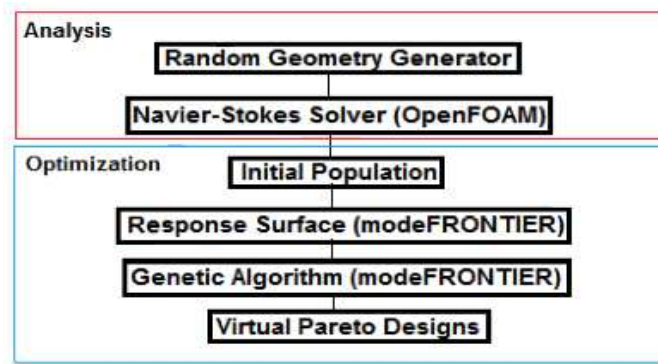


Figure 6: Flow chart showing different software modules

6 RESULTS

Figure 7 shows the initial population used to create the response surface, interpolated (virtual) data on the response surface, and one of the Pareto optimized designs obtained using the NSGA-II algorithm in modeFRONTIER.

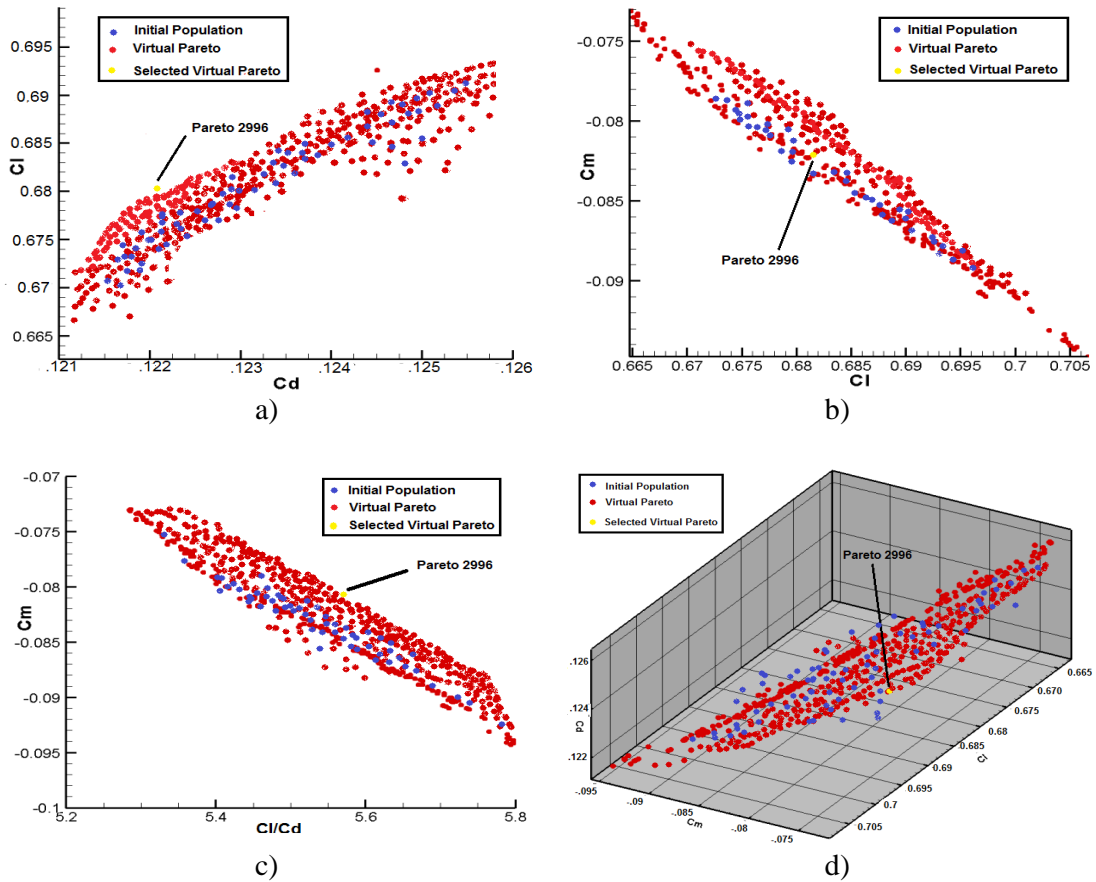
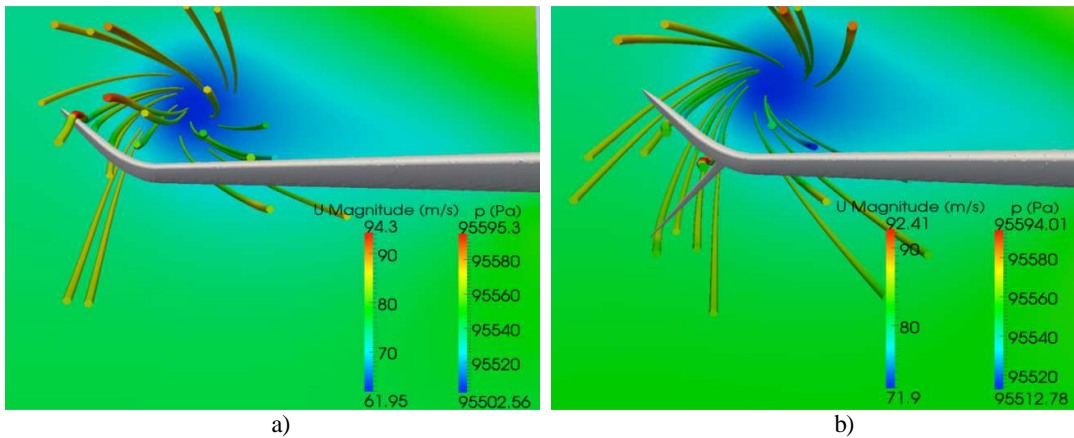


Figure 7: Response surface points for: a) coefficient of lift vs. coefficient of drag, b) coefficient of moment vs. coefficient of lift, c) coefficient of moment vs. lift-to-drag ratio, and d) objective function space made of coefficient of moment vs. coefficient of lift vs. coefficient of drag with initial and virtual wing+winglet data

Table 2: Pareto optimized values of eight design variables defining the scimitar winglet configuration

Design Variable	Value
Upper Leading Edge Sweep	38°
Upper Trailing Edge Sweep	68°
Upper Cant Angle	50°
Upper λ	0.33
Lower Leading Edge Sweep	42°
Lower Trailing Edge Sweep	76°
Lower Cant Angle	68°
Lower λ	0.86

As this study analyzes a winglet design featuring two new additions, the scimitar streamwise spikes, and the secondary lower element, it would be beneficial to analyze the performance enhancement due to each of these components. Figures 8a and 8b show the blended winglet geometry and the blended-ventral strake combination. In Figure 8b, the blended-ventral strake combination does not feature the scimitar spikes. The blended winglet configuration, in Figure 8a shows very strong vortices with very small core, while the blended-ventral strake combination, in Figure 8b, shows a much larger core leading to less induced drag. This is also evident in their respective objective functions (Table 3).



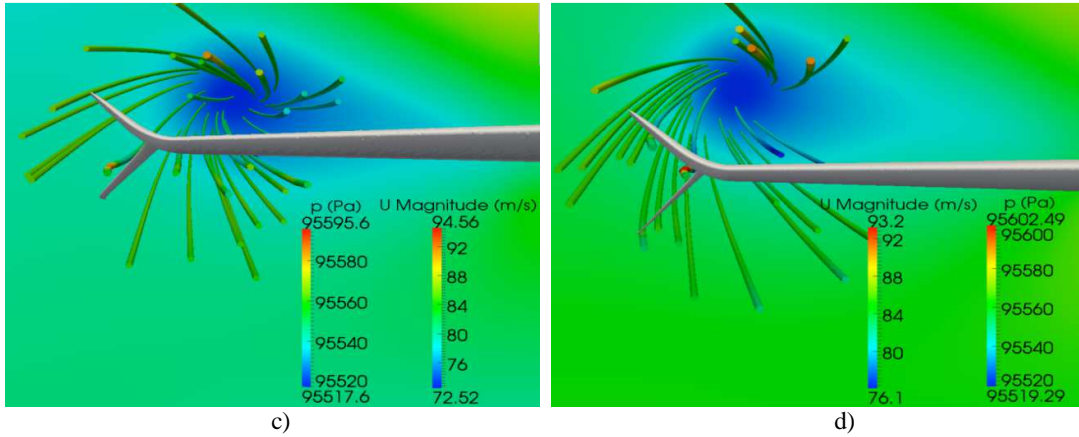


Figure 8: Streamlines at four chord lengths downstream of trailing edge around: a) blended winglet, b) split winglet with no scimitar streamwise spike, c) a non-optimized split winglet with scimitar streamline spike, and d) a Pareto optimized split winglet with scimitar streamwise spike.

From Table 3 it is clear that optimized scimitar split-winglets with streamwise tip spikes offer significant increase of lift and lift-to-drag ratio, while simultaneously lowering aerodynamic drag and significantly lowering aerodynamic moment.

Table 3: Objective function values and percentage improvements for various wing+winglet configurations

Configurations Evaluated	C_L	ΔC_L %	C_D	ΔC_D %	C_m	ΔC_m %	C_L/C_D	$\Delta(C_L/C_D)$ %
Naked Boeing 7E7 wing without winglets	0.6510	0	0.1310	0	-0.121	0	4.97	0
Pareto optimized standard blended winglet	0.6732	3.41	0.1252	-4.43	-0.0932	-22.97	5.38	8.25
An initial (non-optimized) split winglet configuration	0.6750	3.68	0.1240	-5.34	-0.103	-14.87	5.44	9.45
Pareto optimized split winglet without tip spikes	0.6916	6.23	0.1239	-5.73	-0.0870	-28.10	5.58	11.23
Pareto 2996 case optimized split winglet with tip spikes	0.6936	6.54	0.1218	-7.02	-0.0830	-31.40	5.69	14.48

Figures 9 and 10 further demonstrate that these aerodynamic improvements achieved for a specified angle of attack hold also over a range of angles of attack.

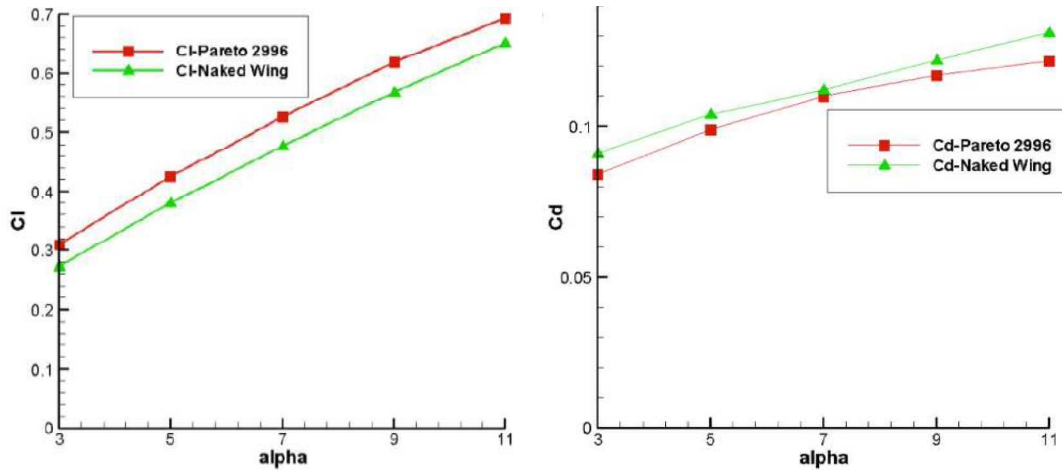


Figure 9: Variations of coefficients of lift and drag as functions of angle of attack for the naked 7E7 wing and for the Pareto optimized 2996 case of wing+scimitar winglet with tip spikes.

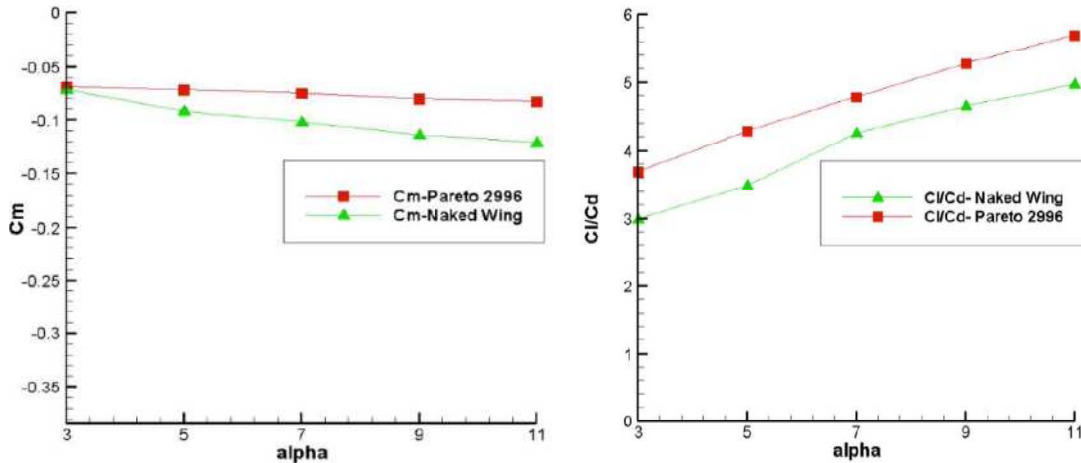


Figure 10: Variations of coefficients of moment and lift-to-drag as functions of angle of attack for the naked 7E7 wing and for the Pareto optimized wing+scimitar winglet with tip spikes.

7 CONCLUSIONS

In this paper, split winglet designs featuring scimitar tip spikes have been investigated using a 3D, compressible Navier-Stokes solver (OpenFOAM). The effects of each individual component of the optimum winglet configuration have been investigated.

Multi-objective optimization was performed on the split winglet configuration. The cant angle, leading and trailing edge sweeps, and length of scimitar spikes for both elements, were the eight design variables for optimization. The four simultaneous objectives of this effort were: maximizing coefficient of lift and lift-to-drag ratio, while minimizing the coefficients of

aerodynamic drag and moment. A multi-dimensional response surface was created using Gaussian Radial Basis Functions (GRBF) as a means to quickly evaluate objective functions for each virtual geometric design. The response surface was coupled with a genetic algorithm (NSGA-II) to perform the optimization. Ten virtual designs were selected from modeFRONTIER and analyzed using Navier-Stokes solver. The interpolated objective function values from the response surface are in good agreement with those obtained from the Navier-Stokes solver.

Results showed that a split winglet configuration diffuses the vortex core more effectively than a simple blended (horns up) winglet. The split winglet configuration with the addition of scimitar tip spikes further increases the wing tip vortex core radius and better redirected the flow to reduce the induced drag. The Pareto optimized configuration was shown to have superior aerodynamic features over a range of aerodynamic angles of attack. That is, consistently lower drag and considerably lower moment, while having consistently higher lift and lift-to-drag ratio. This opens a possibility of optimizing split winglets with multiple elements mimicking a soaring bird's wing tip spread feathers.

ACKNOWLEDGMENTS

The authors would like to express their appreciation to Prof. Carlo Poloni, founder and president of ESTECO, for providing modeFRONTIER optimization software free of charge for this project.

REFERENCES

- [1]. Hossain, A., Rahman, A., Hossen, J., Iqbal, P., Shaari, N. and Sivaraj, G.K., Drag reduction in a wing model using a bird feather like winglet, *Jordan Journal of Mechanical and Industrial Engineering*, Volume 5, Number 3, June 2011.
- [2]. McCormick, B.W. *Aerodynamics of V/STOL Flight*. Academic Press, London, 1967.
- [3]. Louis, B.G. *Spiroid-Tipped Wing*, U. S. patent 5, 102,068, 1992.
- [4]. Smith, M.J., Komerath, N., Ames, R., Wong, O. and Pearson, J. Performance analysis of a wing with multiple winglets, AIAA 19th Applied Aerodynamics Conference, Anaheim, CA, AIAA-2001-2407, 2001.
- [5]. Shelton, A., Tomar, A., Prasad, J.V.R. and Smith, M.J. *et al.*, Active multiple winglets for improved UAV performance, 22nd Applied Aerodynamics Conference and Exhibit, 16 - 19 August, Providence, RI, AIAA 2004-4968, 2004.
- [6]. Alford, L.D. Jr. and Clayman, G.J. Jr., *Blended Winglet*. US Patent 7,644,892, 2010.
- [7]. Kubrynski, K. Wing-winglet design methodology for low speed applications, AIAA paper 03-0215, 41st Aerospace Science Meeting and Exhibit, Reno, NV, January 2003.
- [8]. Bourdin, P., Gatto, A. and Friswell, M.I. The application of variable cant angle winglets for morphing aircraft control, 24th AIAA Applied Aerodynamics Conference, San Francisco, CA, June 5-8, 2006.
- [9]. Ursache, N.M., Melin, T., Isikveren, A.T. and Friswell, M.I. Morphing winglets for aircraft multi-phase improvements, 7th AIAA Aviation Technology, Integration and Operations Conference, Belfast, North Ireland, September 18-20, 2007.
- [10]. Takenaka, K., Hatanaka, K. and Nakahashi, K. Multi-disciplinary design exploration for

- winglet, 26th International Congress of the Aeronautical Sciences, Anchorage, Alaska, USA, September 14-19, 2008.
- [11]. Weierman, J. and Jacob, J.D. Winglet design and optimization for UAVs, AIAA Applied Aerodynamics Conference, June 28 - July 1, 2010.
- [12]. EnginSoft-Newsletter year 7n1, Assesment of optimization algorithms for winglet design, 2010.
- [13]. Minella, G., Ugas, A. and Y. Rodriguez, Aerodynamic shape design optimization of airplane winglets, Senior year B.Sc. thesis, MME Dept., Florida International University, Miami, FL, December 2010.
- [14]. OpenCFD Ltd. OpenFOAM., <http://www.opencfd.co.uk/openfoam/>, 2000-2013.
- [15]. modeFRONTIER optimization software <http://www.esteco.com>
- [16]. Colaço, J.M. and Dulikravich, G.S. A survey of basic deterministic, heuristic and hybrid methods for single-objective optimization and response surface generation, Ch. 10 in *Thermal Measurements and Inverse Techniques*, (ed: Orlande, H.R.B., Fudym, O., Maillet, D. and Cotta, R.), Taylor & Francis, pp. 355-405, May 2011.
- [17]. Klein, M. and Sobieczky, H. Sensitivity of aerodynamic optimization to parameterized target functions. In: M. Tanaka, G.S. Dulikravich, (eds.), *Inverse Problems in Engineering Mechanics*, Elsevier Science, UK, 2001.
- [18]. Sobieczky, H. Geometry generator for CFD and applied aerodynamics. In: *New Design Concepts for High Speed Air Transport*. CISM Courses and Lectures No. 366, Springer, Wien, NewYork, pp. 137 – 157, 1997.
- [19]. Sobol, I.M. Distribution of points in a cube and approximate evaluation of integrals, *U.S.S.R Comput. Maths. Math. Phys*, **7**, pp. 86–112, 1967.
- [20]. Abdoli, A. and Dulikravich, G.S. Optimized multi-floor throughflow micro heat exchangers, *International Journal of Thermal Sciences*, **78**, pp. 111-123, April 2014.
- [21]. Colaco, M. and Dulikravich, G.S. Hybrid optimization algorithms and hybrid response surfaces, (*Plenary Lecture*), Eurogen2013, Las Palmas de Gran Canaria, Spain, October 7-9, 2013.
- [22]. Deb, K., Pratap, A., Agarwal, S. and Meyarivan, T. A fast and elitist multi-objective genetic algorithm- NSGA-II, KanGAL Report Number 2000001, 2000.
- [23]. Deb, K. and Agrawal, R.B. Simulated binary crossover for continuous search space, *Complex Systems*, **9**, pp. 115, 1995.